Adapting a trapped ion mobility spectrometry-Q-TOF for native mass spectrometry

Yu-Fu Lin,[1,2] Benjamin J. Jones,[3] Mark E. Ridgeway,[3] Erin M. Panczyk,[3] Arpad Somogyi,[1,2] Desmond A. Kaplan,[4] Ila Marathe, [1,2] Sangho Yun,[5] Arthur D. Laganowsky,[5] Melvin A. Park,*[3] Vicki Wysocki*[1,2]

1. Department of Chemistry and Biochemistry, The Ohio State University, Columbus, OH

2. Resource for Native MS Guided Structural Biology, The Ohio State University, Columbus, OH

3. Bruker Daltonics Inc., Billerica, MA

4. KapScience LLC, Tewksbury, MA

5. Department of Chemistry, Texas A&M University, College Station, TX

*Corresponding author: wysocki.11@osu.edu and Mel.Park@bruker.com

TOC

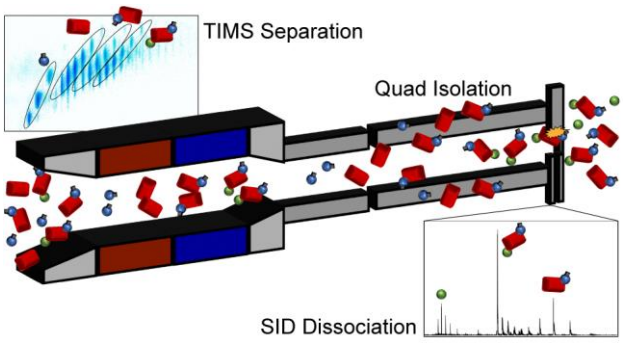

Abstract

Native mass spectrometry (nMS) is increasingly popular for studying intact protein quaternary structure. When coupled with ion mobility, which separates ions based on their size, charge, and shape, it provides additional structural information on the protein complex of interest. In this study, we present a novel prototype TIMS (trapped ion mobility)-Quadrupole-SID (surface-induced dissociation)-Time of Flight (TIMS-Q-SID-TOF) instrument for nMS. The modifications include changing the TIMS cartridge from concave to convex geometry electrodes and operating TIMS at 425 kHz to improve the trapping efficiency for high mass-to-charge (*m/z*) ion mobility analysis, such as 3 and 4 MDa hepatitis B virus capsids. The quadrupole radiofrequency driver was lowered to 385 kHz, which extends the isolation range from 3,000 to 17,000 *m/z* and allows isolation of a single charge state of GroEL at 16,200 *m/z* with an isolation window of 25 *m/z*. Finally, a 6-mm thick, 2-lens SID device was installed and replaced the collision cell entrance lens. The SID dissociated 801 kDa GroEL into all combinations of subcomplexes, and the peaks were well-resolved and easy to interpret. This is the first time a novel prototype timsTOF Pro for nMS has been introduced with high resolving power ion mobility separation coupled to high *m/z* quadrupole selection

and SID for protein complex fragmentation with product ion collection across a broad *m/z* range of 1,500 to 40,000.

Introduction

Trapped ion mobility spectrometry (TIMS) is a high-resolution ion mobility spectrometry technique that was first introduced by Park and co-workers in 2011.[1,2] Unlike the traditional drift tube ion mobility cell (DTIMS), which uses ions flying through a stationary gas in the drift tube, TIMS separates ions by using an electric field and a moving column of gas to measure the analyte's ion mobility.[3] TIMS has been coupled to a Q-TOF mass spectrometer and is widely applied in proteomics and metabolomics, including cross-linking mass spectrometry.[4–9] Recently, Panczyk et al. demonstrated that a commercial TIMS-Q-TOF can perform nMS analysis on protein complexes up to 100 kDa.[10] Borotto and co-workers showed that commercial TIMS-Q-TOF could also characterize protein structure up to 66 kDa by top-down sequencing and collision-induced unfolding by activation within the TIMS device.[11–13] Fernandez-Lima and co-workers reported that the modified convex TIMS cartridge with a low radio frequency (RF) driver improves the ion mobility analysis of TIMS up to 800 kDa with a single peak resolution (R_p) of 85 compared to DTIMS with an R_p of 60 for protein complexes around or above 200 kDa.[14–16] Because nMS use is continuing to expand[17–21], and coupling it with IMS provides additional protein and protein complex structural information[22–24], we aimed in the work reported here to adapt TIMS[1–3,25] to perform nMS for studying and understanding large, complex protein structures up to the mega-Dalton (MDa) range with a high energy deposition tandem mass spectrometry (MS/MS) activation method, surface-induced dissociation (SID).[26–29] The Wysocki lab has extended SID development to investigate protein structure and subcomplex connectivity for macromolecules.[27,30–32] SID cleaves protein complexes at their weakest non-covalent interfaces and generates subunits with a charge state approximately proportional to the relative fragment ion mass.[30,33] Currently, nMS has been applied to measure macromolecules in the MDa mass range, such as adeno-associated virus capsids (3.5 – 5 MDa), antibody-bound capsids species (5 – 17 MDa), and oligomerized 20S proteasome (0.7 – 9.6 MDa).[34–37] The Wysocki lab has demonstrated the application of SID, the only MS/MS that extensively dissociates MDa biomolecules, to investigate the structure of AAVs.[38]

Here, we modified a commercial TIMS-Q-TOF mass spectrometer to study structures of high molecular weight (MW) protein complexes. The modifications include changing the TIMS cartridge geometry to convex, lowering the RF frequency for both the TIMS device and quadrupole, and installing a 2-lens SID device.[39] With these novel modifications, the application of nMS with ion mobility and SID on this prototype platform ranges from 50 kDa to at least 4 MDa.

Experimental Section

Materials and Sample Preparation. More details on materials and selected protein complexes can be found in Supporting Information. All protein complexes were buffer exchanged into 200 mM ammonium acetate using size exclusion chromatography spin columns (Bio-Rad) with a 6 kDa mass cutoff and charge-reduced using 20% (v/v) triethylammonium acetate (TEAA) because we have found that lower charge state precursors of protein complexes give more native-like fragmentation patterns by SID in general. Typically, the sample concentration for analysis was in the range of 0.7 to 3 µM per complex after dilution and charge reduction. For T3 and T4 hepatitis B virus capsids (HBV), the concentration was 6 µM per monomer and 4.8 µM per monomer after charge reduction. For the RAS-SOS complex analysis, 3 µM SOS

was mixed with 2 µM HRasWT-GTP and immediately introduced into the mass spectrometer via a pulled glass capillary.

Instrumentation and experiments. Experiments were conducted on a timsTOF Pro (TIMS-Q-TOF) (Bruker Inc., Billerica, MA), modified for the research presented here. A 385 kHz RF frequency quadrupole driver was installed to extend the quadrupole isolation range from 3,000 *m/z* with a commercial 1 MHz RF frequency quadrupole driver to 17,000 *m/z*. Here, we used protein complexes for calibration and calibrated the quadrupole up to 12,000 *m/z*, which can isolate a single charge state at 16,200 *m/z* with an isolation width of 25 *m/z* (Figure S1). In general operation, the "TIMS In" pressure was reduced to 2.2 mbar. The "Accumulation time" and "Ramp Time" of the TIMS device were adjusted to 100.0 ms and 1,000.0 ms (10.00 % Duty Cycle), respectively. The "Funnel 1 RF" was 300.0 volt peak-to-peak (V_{pp}). The "Collision Cell In", which determines the *m/z* transferring range, was 150.0 V. The "Pre Pulse Storage", a delay for collecting ions between "Transfer Time" and "TOF Pulser On", was 35.0 µs. "Pre Pulse Storage" functions as a low mass limit. Lowering "Pre Pulse Storage" can transfer small ions to the TOF. The "Transfer Time" is the time corresponding to transmitting ions to the TOF stage and was set to 140.0, 320.0, and 520.0 µs depending on the size of the protein complex. Increasing the "Transfer Time" can transfer larger ions to the TOF. The "Collision Gas Flow Rate" was 35.0 % for the ESI Tuning Mix and 88.0 % for protein complexes. The default "Delta Values", which control TIMS parameters (Figure S2), was used for all the experiments. More details of the typical settings for nMS can be found in the Supporting Information (Table S1).

All samples were ionized and introduced using a custom Bruker nanoelectrospray ionization source. The instrument was mass calibrated using ESI Tuning Mix. The SID experiments were conducted with or without single charge state isolation using the quadrupole, as noted in the Results section, and the SID potentials were varied appropriately to initiate the fragmentation of different sizes of chosen analytes (Supporting Information shows the tuning and operation of SID). For pre-ion mobility ion activation experiments, the *Δt6* value was run from 10.0 to 200.0 V.[12,40] The instrument was operated using Bruker's otofControl 6.2 software, and the data were analyzed using DataAnalysis 5.3.

Results and Discussions

To evaluate the performance of the modified instrument (Figure 1), several model protein complexes, including 53 kDa homotetrameric streptavidin (SA), 64 kDa homotetrameric avidin (AV), 103 kDa homotetrameric concanavalin A (Con A), 147 kDa homotetrameric alcohol dehydrogenase (ADH), 58 kDa homopentameric cholera toxin B (CTB), 115 kDa homopentameric C-reactive protein (CRP), 90 kDa heterohexameric his-tagged toyocamycin nitrile hydratase (His-TNH), 801 kDa wild-type 14-mer GroEL, and 3 MDa T3 and 4 MDa T4 HBVs, were chosen and are discussed below.[30,35,41,42] HRas*GTP-SOS-HRas complex was used to evaluate TIMS-Q-SID performance.[43]

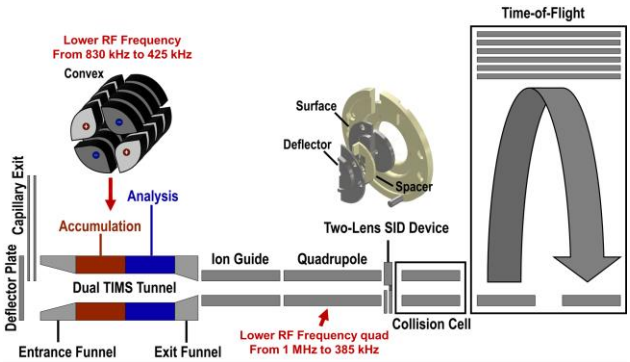

Figure 1. The instrument diagram of the modified Bruker timsTOF Pro. The TIMS cartridge has convex geometry electrodes and is operated at 425 kHz. The quadrupole is operated at 385 kHz to extend the isolation range to 17,000 *m/z*. The 2-lens SID device replaces the entrance lens of the collision cell.

Extending the Mass-to-charge Ratio Range for Protein Complex Ion Mobility Analysis. Initially, the TIMS-Q-TOF instrument was configured with a concave TIMS cartridge (Figure S3a) with an 830 kHz RF TIMS driver, which can trap ions up to 6,000 *m/z*.[10] In the work described here, the TIMS cartridge was changed to a convex electrode geometry (inset of Figure 1 and Figure S3b) coupled with a 425 kHz RF frequency TIMS driver to enhance the trapping efficiency for species up to 38,000 *m/z*. The performance of the TIMS device with convex electrodes was verified with selected model protein complexes, which ranged in mass from 50 – 801 kDa (4,500 – 18,500 *m/z*).

To test the effective *m/z* range of this modified TIMS device, lower-mass complexes and 180-mer T3 and 240-mer T4 HBV capsids, with masses of ~3 MDa and ~4 MDa, respectively, were investigated.[35,44] The mobility peaks for different charge states of lower-mass complexes, SA and ADH, were mostly baseline resolved (Figure S4). Figure 2a shows the MS spectrum of T3 and T4 HBV. With the modified TIMS cartridge, T3 and T4 were trapped successfully during the ion mobility analysis (Figure 2b). The *m/z* peaks of each distribution are partially resolved, and the charge states of the central distribution of each HBV can be determined. T3 and T4 were also further charge-reduced with TEAA, and the result is shown in Figure S5. Briefly, we were able to separate the charge-reduced T3 and T4 capsids using this modified TIMS device.

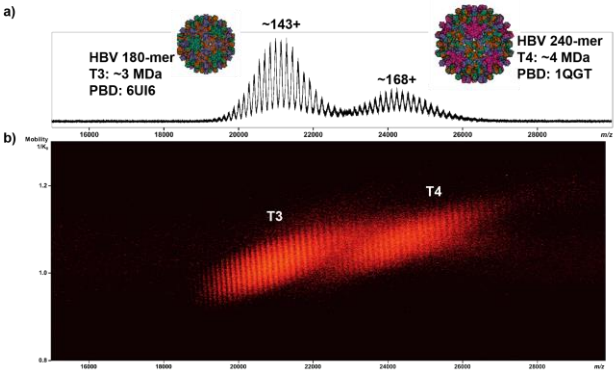

Figure 2. a) The spectrum of ~33 nM 180-mer (T3, ~3 MDa) and ~25 nM 240-mer (T4, ~4 MDa) Hepatitis B virus capsids (~ 6 µM per monomer) in 200 mM ammonium acetate. b) The mobiligram of T3 and T4. The modified TIMS cartridge trapped both T3 and T4 and measured their ion mobilities.

Performance of a Two-lens Surface-induced Dissociation Device. The SID device design on this instrument was inspired by the designs of Snyder et al.[39] The device is simplified to a 2-lens system (inset of Figure 1). The overall width of this device along the ion optical axis is 6 mm, which is the width of the collision cell entrance lens that is removed to make room for the SID device. The SID surface and extractor were combined into a ring electrode with a 3 mm diameter aperture. The deflector is a half-moon-shaped electrode. Both surface and deflector were made with tight-tolerance corrosion-resistant 316 stainless steel. An insulated spacer made of polyether ether ketone (PEEK) material was placed between the surface and the deflector to prevent an electrical short circuit. The device replaced the collision cell entrance lens. The surface was controlled by an existing spare system voltage on the instrument, and the deflector was controlled using the voltage typically supplied to the collision cell entrance lens (Focus 2 L3). To examine the performance of the installed SID device, selected model protein complexes, SA, AV, ADH, ConA, CTB, CRP, and His-TNH, were fragmented by SID, and results are shown in Figure S7.

The largest protein complex fragmented here to test the SID performance was 801 kDa GroEL. We isolated 68+ and 47+ GroEL at 11,850 and 16,950 *m/z*, respectively, with an isolation window of 200 *m/z*, and fragmented them using SID. The SID energies were adjusted to 7,520 eV and 7,480 eV, respectively, to compare their results under an approximately equal SID energy level. Figure 3 shows the SID results from both selected ions. After deconvolving the spectrum using UniDec[45], the results show that, after SID, 47+ GroEL (Figure 3d) has fewer monomers and 13-mers formed, and it is more favorable to produce 7-mers, which reflects a more native-like structure compared to the SID result of 68+ GroEL (Figure 3b).

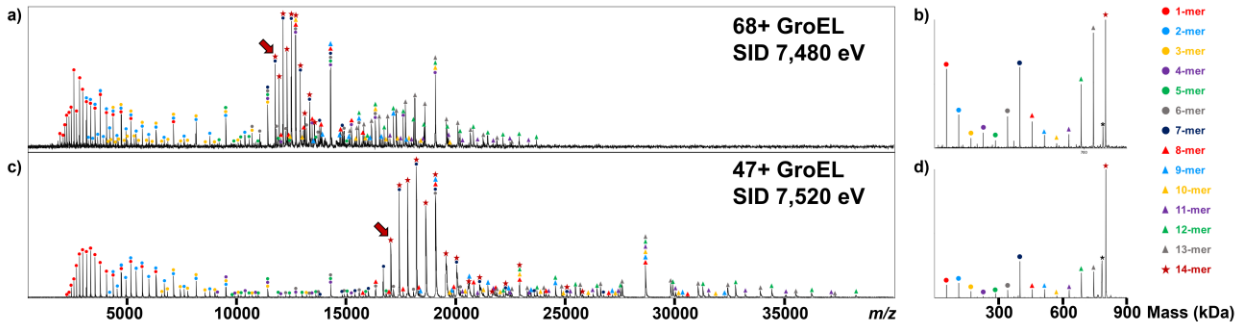

Figure 3. The SID spectra of a) 68+ and b) 47+ GroEL at SID energy 7,480 and 7,520 eV, respectively. The deconvolved mass spectra show the relative abundance of SID products from b) 68+ and c) 47+ GroEL. The red arrows indicate the selected 68+ and 47+ GroEL precursors. The legend shows different subcomplexes of GroEL SID products and their representative symbols. The asterisk represents a deconvolution error. These deconvolution error peaks are assigned from an atypical *m/z* peak distribution (asymmetric peak heights from the centroid peak).

Analysis of a complex mixture using the modified TIMS-Q-TOF. When the sample is a complex mixture, using TIMS to separate the mixture by ion mobility and isolating a narrow *m/z* range of interest before SID makes the identification of SID fragments easier. When the HRas-SOS mixture was ionized, 4 different proteins and protein complexes, HRas*GTP, SOS, HRas*GTP-SOS, and HRas*GTP-SOS-HRas, were observed in the MS1 spectrum (Figure 4a). We were interested in studying the structure of the full HRas*GTP-SOS-HRas complex. However, from the mobiligram shown in Figure 4b, there were always other protein complexes around HRas*GTP-SOS-HRas. To perform SID and characterize the HRas*GTP-SOS-HRas complex, the mixture was first separated using TIMS. We then isolated a narrow *m/z* range of interest, and 16+ HRas*GTP-SOS and 20+ HRas*GTP-SOS-HRas were isolated. These two complexes were then fragmented by SID. To identify the SID fragments of 20+ HRas*GTP-SOS-HRas, we generated the SID spectrum of 20+ HRas*GTP-SOS-HRas by averaging its mobility peak (Figure 4c). The result shows that

HRas*GTP-SOS-HRas dissociates into two species: HRas and HRas*GTP-SOS, and HRas*GTP interacts more strongly with SOS than HRas. It's also interesting to note that HRas carried about half of the charges from the precursor after being dissociated from the complex, which was not anticipated. Typically, SID fragments carry charges proportional to the mass of the precursor.[27,29,32] This suggests that HRas undergoes structural rearrangement to depart from the complex, which is similar to results reported for some complexes.[46] Overall, with the cooperation of TIMS separation and quadrupole isolation, we were able to study the structure of HRas*GTP-SOS-HRas using SID without any interference from other complexes in the mixture.

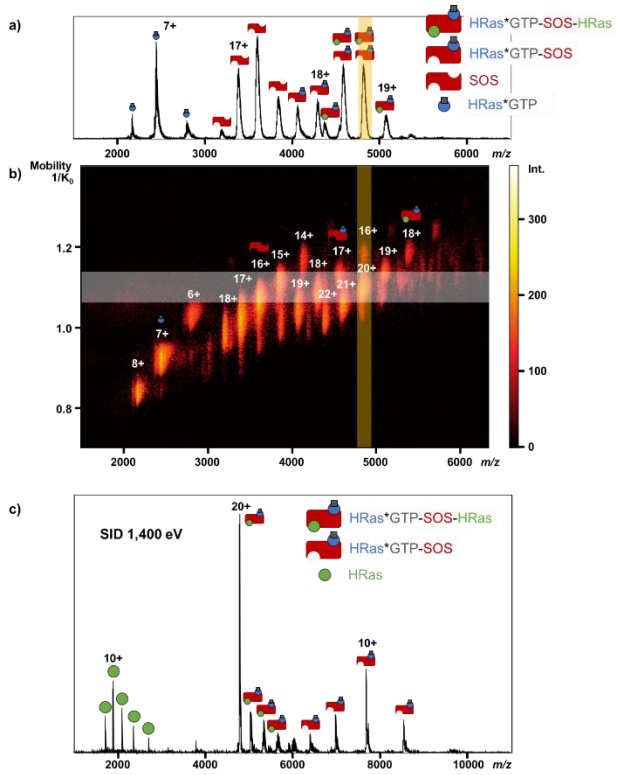

Figure 4 a) The mass spectrum and b) the mobiligram of the HRas-SOS complex. c) The SID result of 20+ HRas*GTP-SOS-HRas at SID 1,400 eV. The shaded yellow area represents the isolation using quadrupoles, while the white area represents the averaging area used to generate the SID spectrum after quadrupole isolation.

Conclusions

Here, we demonstrated that with a low RF frequency convex TIMS device, we are able to mobility-separate charge-reduced 3 and 4 MDa T3 and T4 HBV capsids. A single charge state of charge-reduced GroEL could be selected at *m/z* 16,200 with a 25 *m/z* isolation window with the low RF frequency quadrupole driver. Also, a 2-lens SID device was able to fragment 801 kDa GroEL and investigate its subunit connectivity. Significantly, the peaks of fragments at high *m/z* are well resolved, which improves the identification of different subcomplexes. SID can also be used as a tool to probe the structural information of ions of interest. The detection limit of this instrument is also outstanding. We were able to perform nMS for HBV capsids in the concentration range of 20 to 50 nM. Moreover, with TIMS, when characterizing a specific protein complex from a complex mixture using nMS, we were able to differentiate those SID fragments from others. This simplifies the interpretation of SID products from the complex mixture.

Acknowledgments

We thank Dalton T. Snyder (Resource for Native Mass Spectrometry Guided Structural Biology, OSU) for helpful discussions, Marshell Bern and Ignat Shilov (Protein Metrics, LLC) for the input and discussion of the deconvolved GroEL SID results, and the Ohio State University ASC machine shop for machining SID device parts. We also thank Bandarian lab (University of Utah) for his-tagged toyocamycin nitrile hydratase, the Hayes Rye Group (Texas A&M University) for wild-type GroEL samples, and Karen Kirby and Stefan Sarafianos (Emory University) for T3 and T4 HBV capsids. We gratefully acknowledge funding from the National Institutes of Health (NIH RM1GM149374 to V. H. W.).

Author Information

The authors declare the following competing financial interests: BJJ, MER, EMP, and MAP are employees of Bruker, which manufactures and sells the Bruker timsTOF Pro modified in this work. The work in the Wysocki lab was performed collaboratively with the Bruker team.

Reference

(1) Fernandez-Lima, F.; Kaplan, D. A.; Suetering, J.; Park, M. A. Gas-Phase Separation Using a Trapped Ion Mobility Spectrometer. *Int. J. Ion Mobil. Spec.* **2011**, *14* (2), 93–98. https://doi.org/10.1007/s12127-011-0067-8.

(2) Fernandez-Lima, F. A.; Kaplan, D. A.; Park, M. A. Note: Integration of Trapped Ion Mobility Spectrometry with Mass Spectrometry. *Review of Scientific Instruments* **2011**, *82* (12), 126106. https://doi.org/10.1063/1.3665933.

(3) Ridgeway, M. E.; Lubeck, M.; Jordens, J.; Mann, M.; Park, M. A. Trapped Ion Mobility Spectrometry: A Short Review. *International Journal of Mass Spectrometry* **2018**, *425*, 22–35. https://doi.org/10.1016/j.ijms.2018.01.006.

(4) Ridgeway, M. E.; Bleiholder, C.; Mann, M.; Park, M. A. Trends in Trapped Ion Mobility – Mass Spectrometry Instrumentation. *TrAC Trends in Analytical Chemistry* **2019**, *116*, 324–331. https://doi.org/10.1016/j.trac.2019.03.030.

(5) Lesur, A.; Schmit, P.-O.; Bernardin, F.; Letellier, E.; Brehmer, S.; Decker, J.; Dittmar, G. Highly Multiplexed Targeted Proteomics Acquisition on a TIMS-QTOF. *Anal. Chem.* **2021**, *93* (3), 1383–1392. https://doi.org/10.1021/acs.analchem.0c03180.

(6) Meier, F.; Park, M. A.; Mann, M. Trapped Ion Mobility Spectrometry and Parallel Accumulation–Serial Fragmentation in Proteomics. *Molecular & Cellular Proteomics* **2021**, *20*. https://doi.org/10.1016/j.mcpro.2021.100138.

(7) Aballo, T. J.; Roberts, D. S.; Melby, J. A.; Buck, K. M.; Brown, K. A.; Ge, Y. Ultrafast and Reproducible Proteomics from Small Amounts of Heart Tissue Enabled by Azo and TimsTOF Pro. *J. Proteome Res.* **2021**, *20* (8), 4203–4211. https://doi.org/10.1021/acs.jproteome.1c00446.

(8) Ihling, C. H.; Piersimoni, L.; Kipping, M.; Sinz, A. Cross-Linking/Mass Spectrometry Combined with Ion Mobility on a TimsTOF Pro Instrument for Structural Proteomics. *Anal. Chem.* **2021**, *93* (33), 11442–11450. https://doi.org/10.1021/acs.analchem.1c01317.

(9) Guergues, J.; Wohlfahrt, J.; Stevens, S. M. Jr. Enhancement of Proteome Coverage by Ion Mobility Fractionation Coupled to PASEF on a TIMS–QTOF Instrument. *J. Proteome Res.* **2022**, *21* (8), 2036–2044. https://doi.org/10.1021/acs.jproteome.2c00336.
(10) Panczyk, E.; Lin, Y.-F.; Snyder, D.; Liu, F.; Ridgeway, M.; Park, M.; Bleiholder, C.; Wysocki, V. Evaluation of a Bruker TimsTOF Pro for Native Mass Spectrometry. ChemRxiv September 12, 2023. https://doi.org/10.26434/chemrxiv-2021-qr78t-v2.
(11) Borotto, N. B.; Graham, K. A. Fragmentation and Mobility Separation of Peptide and Protein Ions in a Trapped-Ion Mobility Device. *Anal. Chem.* **2021**, *93* (29), 9959–9964. https://doi.org/10.1021/acs.analchem.1c01188.
(12) Borotto, N. B.; Osho, K. E.; Richards, T. K.; Graham, K. A. Collision-Induced Unfolding of Native-like Protein Ions Within a Trapped Ion Mobility Spectrometry Device. *J. Am. Soc. Mass Spectrom.* **2022**, *33* (1), 83–89. https://doi.org/10.1021/jasms.1c00273.
(13) Graham, K. A.; Lawlor, C. F.; Borotto, N. B. Characterizing the Top-down Sequencing of Protein Ions Prior to Mobility Separation in a TimsTOF. *Analyst* **2023**, *148* (7), 1534–1542. https://doi.org/10.1039/d2an01682f.
(14) McCabe, J. W.; Mallis, C. S.; Kocurek, K. I.; Poltash, M. L.; Shirzadeh, M.; Hebert, M. J.; Fan, L.; Walker, T. E.; Zheng, X.; Jiang, T.; Dong, S.; Lin, C.-W.; Laganowsky, A.; Russell, D. H. First-Principles Collision Cross Section Measurements of Large Proteins and Protein Complexes. *Anal Chem* **2020**, *92* (16), 11155–11163. https://doi.org/10.1021/acs.analchem.0c01285.
(15) France, A. P.; Migas, L. G.; Sinclair, E.; Bellina, B.; Barran, P. E. Using Collision Cross Section Distributions to Assess the Distribution of Collision Cross Section Values. *Anal. Chem.* **2020**, *92* (6), 4340–4348. https://doi.org/10.1021/acs.analchem.9b05130.
(16) Jeanne Dit Fouque, K.; Garabedian, A.; Leng, F.; Tse-Dinh, Y.-C.; Ridgeway, M. E.; Park, M. A.; Fernandez-Lima, F. Trapped Ion Mobility Spectrometry of Native Macromolecular Assemblies. *Anal. Chem.* **2021**, *93* (5), 2933–2941. https://doi.org/10.1021/acs.analchem.0c04556.
(17) Zhou, M.; Lantz, C.; A. Brown, K.; Ge, Y.; Paša-Tolić, L.; A. Loo, J.; Lermyte, F. Higher-Order Structural Characterisation of Native Proteins and Complexes by Top-down Mass Spectrometry. *Chemical Science* **2020**, *11* (48), 12918–12936. https://doi.org/10.1039/D0SC04392C.
(18) Ruotolo, B. T.; Marty, M. T. Native Mass Spectrometry for Structural Biology: A Perspective. *International Journal of Mass Spectrometry* **2021**, *468*, 116655. https://doi.org/10.1016/j.ijms.2021.116655.
(19) Campuzano, I. D. G.; Sandoval, W. Denaturing and Native Mass Spectrometric Analytics for Biotherapeutic Drug Discovery Research: Historical, Current, and Future Personal Perspectives. *J. Am. Soc. Mass Spectrom.* **2021**, *32* (8), 1861–1885. https://doi.org/10.1021/jasms.1c00036.
(20) Tamara, S.; den Boer, M. A.; Heck, A. J. R. High-Resolution Native Mass Spectrometry. *Chem. Rev.* **2022**, *122* (8), 7269–7326. https://doi.org/10.1021/acs.chemrev.1c00212.
(21) Rolland, A. D.; Prell, J. S. Approaches to Heterogeneity in Native Mass Spectrometry. *Chem. Rev.* **2022**, *122* (8), 7909–7951. https://doi.org/10.1021/acs.chemrev.1c00696.
(22) Konijnenberg, A.; Butterer, A.; Sobott, F. Native Ion Mobility-Mass Spectrometry and Related Methods in Structural Biology. *Biochimica et Biophysica Acta (BBA) - Proteins and Proteomics* **2013**, *1834* (6), 1239–1256. https://doi.org/10.1016/j.bbapap.2012.11.013.
(23) Allison, T. M.; Barran, P.; Cianférani, S.; Degiacomi, M. T.; Gabelica, V.; Grandori, R.; Marklund, E. G.; Menneteau, T.; Migas, L. G.; Politis, A.; Sharon, M.; Sobott, F.; Thalassinos, K.; Benesch, J. L. P. Computational Strategies and Challenges for Using Native Ion Mobility Mass Spectrometry in Biophysics and Structural Biology. *Anal. Chem.* **2020**, *92* (16), 10872–10880. https://doi.org/10.1021/acs.analchem.9b05791.

(24) McCabe, J. W.; Hebert, M. J.; Shirzadeh, M.; Mallis, C. S.; Denton, J. K.; Walker, T. E.; Russell, D. H. The Ims Paradox: A Perspective on Structural Ion Mobility-Mass Spectrometry. *Mass Spectrometry Reviews* **2021**, *40* (3), 280–305. https://doi.org/10.1002/mas.21642.
(25) Ridgeway, M.; Woods, L.; Park, M. CHAPTER 5:Trapped Ion Mobility Spectrometry – Basics and Calibration. In *Ion Mobility-Mass Spectrometry*; 2021; pp 105–131. https://doi.org/10.1039/9781839162886-00105.
(26) Morris, M. R.; Riederer, D. E.; Winger, B. E.; Cooks, R. G.; Ast, T.; Chidsey, C. E. D. Ion/Surface Collisions at Functionalized Self-Assembled Monolayer Surfaces. *International Journal of Mass Spectrometry and Ion Processes* **1992**, *122*, 181–217. https://doi.org/10.1016/0168-1176(92)87016-8.
(27) Stiving, A. Q.; VanAernum, Z. L.; Busch, F.; Harvey, S. R.; Sarni, S. H.; Wysocki, V. H. Surface-Induced Dissociation: An Effective Method for Characterization of Protein Quaternary Structure. *Anal. Chem.* **2019**, *91* (1), 190–209. https://doi.org/10.1021/acs.analchem.8b05071.
(28) Snyder, D. T.; Harvey, S. R.; Wysocki, V. H. Surface-Induced Dissociation Mass Spectrometry as a Structural Biology Tool. *Chem. Rev.* **2021**, acs.chemrev.1c00309. https://doi.org/10.1021/acs.chemrev.1c00309.
(29) Karch, K. R.; Snyder, D. T.; Harvey, S. R.; Wysocki, V. H. Native Mass Spectrometry: Recent Progress and Remaining Challenges. *Annual Review of Biophysics* **2022**, *51* (1), null. https://doi.org/10.1146/annurev-biophys-092721-085421.
(30) Harvey, S. R.; Seffernick, J. T.; Quintyn, R. S.; Song, Y.; Ju, Y.; Yan, J.; Sahasrabuddhe, A. N.; Norris, A.; Zhou, M.; Behrman, E. J.; Lindert, S.; Wysocki, V. H. Relative Interfacial Cleavage Energetics of Protein Complexes Revealed by Surface Collisions. *PNAS* **2019**, *116* (17), 8143–8148. https://doi.org/10.1073/pnas.1817632116.
(31) Harvey, S. R.; Liu, Y.; Liu, W.; Wysocki, V. H.; Laganowsky, A. Surface Induced Dissociation as a Tool to Study Membrane Protein Complexes. *Chem. Commun.* **2017**, *53* (21), 3106–3109. https://doi.org/10.1039/C6CC09606A.
(32) Snyder, D. T.; Jones, B. J.; Lin, Y.-F.; Cooper-Shepherd, D. A.; Hewitt, D.; Wildgoose, J.; Brown, J. M.; Langridge, J. I.; Wysocki, V. H. Surface-Induced Dissociation of Protein Complexes on a Cyclic Ion Mobility Spectrometer. *Analyst* **2021**, *146* (22), 6861–6873. https://doi.org/10.1039/D1AN01407B.
(33) Wang, J.; Meroueh, S. O.; Wang, Y.; Hase, W. L. Efficiency of Energy Transfer in Protonated Diglycine and Dialanine SID: Effects of Collision Angle, Peptide Ion Size, and Intramolecular Potential. *International Journal of Mass Spectrometry* **2003**, *230* (1), 57–63. https://doi.org/10.1016/j.ijms.2003.08.005.
(34) Barnes, L. F.; Draper, B. E.; Jarrold, M. F. Analysis of Recombinant Adenovirus Vectors by Ion Trap Charge Detection Mass Spectrometry: Accurate Molecular Weight Measurements beyond 150 MDa. *Anal. Chem.* **2022**, *94* (3), 1543–1551. https://doi.org/10.1021/acs.analchem.1c02439.
(35) Uetrecht, C.; Versluis, C.; Watts, N. R.; Roos, W. H.; Wuite, G. J. L.; Wingfield, P. T.; Steven, A. C.; Heck, A. J. R. High-Resolution Mass Spectrometry of Viral Assemblies: Molecular Composition and Stability of Dimorphic Hepatitis B Virus Capsids. *Proceedings of the National Academy of Sciences* **2008**, *105* (27), 9216–9220. https://doi.org/10.1073/pnas.0800406105.
(36) Grande, A. E.; Li, X.; Miller, L. M.; Zhang, J.; Draper, B. E.; Herzog, R. W.; Xiao, W.; Jarrold, M. F. Antibody Binding to Recombinant Adeno Associated Virus Monitored by Charge Detection Mass Spectrometry. *Anal. Chem.* **2023**, *95* (29), 10864–10868. https://doi.org/10.1021/acs.analchem.3c02371.
(37) Anthony, A. J.; Gautam, A. K. S.; Miller, L. M.; Ma, Y.; Hardwick, A. G.; Sharma, A.; Ghatak, S.; Matouschek, A.; Jarrold, M. F.; Clemmer, D. E. CDMS Analysis of Intact 19S, 20S, 26S, and 30S Proteasomes: Evidence for Higher-Order 20S Assemblies at a Low PH. *Anal. Chem.* **2023**, *95* (33), 12209–12215. https://doi.org/10.1021/acs.analchem.3c00472.

(38) Du, C.; Cleary, S. P.; Kostelic, M. M.; Jones, B. J.; Kafader, J. O.; Wysocki, V. H. Combining Surface-Induced Dissociation and Charge Detection Mass Spectrometry to Reveal the Native Topology of Heterogeneous Protein Complexes. *Anal. Chem.* **2023**, *95* (37), 13889–13896. https://doi.org/10.1021/acs.analchem.3c02185.
(39) Snyder, D. T.; Panczyk, E. M.; Somogyi, A.; Kaplan, D. A.; Wysocki, V. Simple and Minimally Invasive SID Devices for Native Mass Spectrometry. *Anal. Chem.* **2020**, *92* (16), 11195–11203. https://doi.org/10.1021/acs.analchem.0c01657.
(40) Liu, F. C.; Ridgeway, M. E.; Winfred, J. S. R. V.; Polfer, N. C.; Lee, J.; Theisen, A.; Wootton, C. A.; Park, M. A.; Bleiholder, C. Tandem-Trapped Ion Mobility Spectrometry/Mass Spectrometry Coupled with Ultraviolet Photodissociation. *Rapid Communications in Mass Spectrometry* **2021**, *35* (22), e9192. https://doi.org/10.1002/rcm.9192.
(41) Zhou, M.; Jones, C. M.; Wysocki, V. H. Dissecting the Large Noncovalent Protein Complex GroEL with Surface-Induced Dissociation and Ion Mobility–Mass Spectrometry. *Anal. Chem.* **2013**, *85* (17), 8262–8267. https://doi.org/10.1021/ac401497c.
(42) Quintyn, R. S.; Zhou, M.; Yan, J.; Wysocki, V. H. Surface-Induced Dissociation Mass Spectra as a Tool for Distinguishing Different Structural Forms of Gas-Phase Multimeric Protein Complexes. *Anal. Chem.* **2015**, *87* (23), 11879–11886. https://doi.org/10.1021/acs.analchem.5b03441.
(43) Yun, S. D.; Scott, E.; Moghadamchargari, Z.; Laganowsky, A. 2'-Deoxy Guanosine Nucleotides Alter the Biochemical Properties of Ras. *Biochemistry* **2023**, *62* (16), 2450–2460. https://doi.org/10.1021/acs.biochem.3c00258.
(44) Uetrecht, C.; Barbu, I. M.; Shoemaker, G. K.; van Duijn, E.; Heck, A. J. R. Interrogating Viral Capsid Assembly with Ion Mobility-Mass Spectrometry. *Nat Chem* **2011**, *3* (2), 126–132. https://doi.org/10.1038/nchem.947.
(45) Kostelic, M. M.; Zak, C. K.; Liu, Y.; Chen, V. S.; Wu, Z.; Sivinski, J.; Chapman, E.; Marty, M. T. UniDecCD: Deconvolution of Charge Detection-Mass Spectrometry Data. *Anal. Chem.* **2021**, *93* (44), 14722–14729. https://doi.org/10.1021/acs.analchem.1c03181.
(46) Sahasrabuddhe, A.; Hsia, Y.; Busch, F.; Sheffler, W.; King, N. P.; Baker, D.; Wysocki, V. H. Confirmation of Intersubunit Connectivity and Topology of Designed Protein Complexes by Native MS. *Proceedings of the National Academy of Sciences* **2018**, *115* (6), 1268–1273. https://doi.org/10.1073/pnas.1713646115.